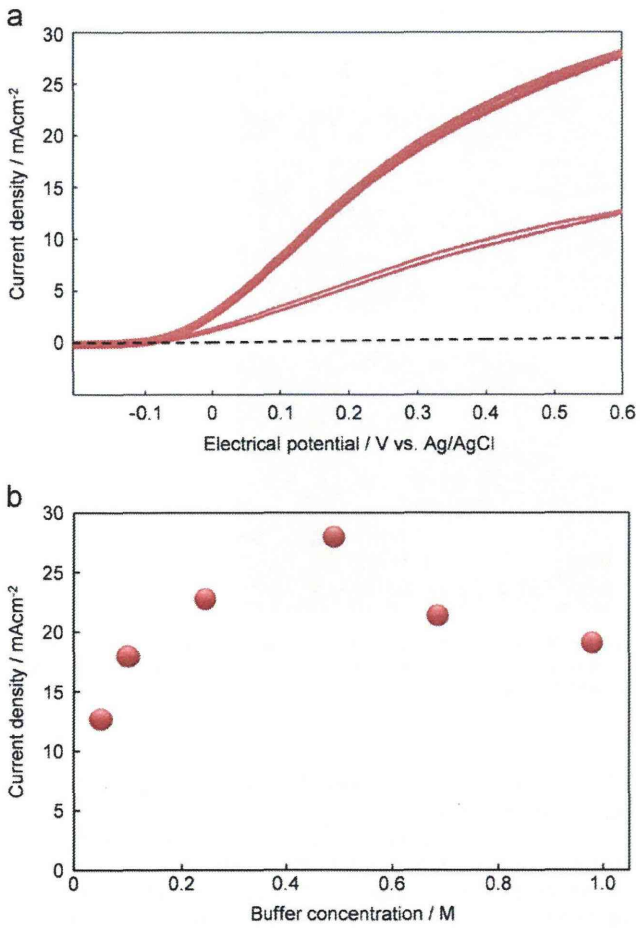

Fig. 2. (a) Cyclic voltammograms of fructose oxidation at 10 mV s^{-1} in a stirred 50 mM buffer solution (pH 5) containing 500 mM fructose. The CF strip electrodes were modified with only 10 mg ml^{-1} FDH (broken black line) or with both 10 mg ml^{-1} CNT and 10 mg ml^{-1} FDH (red line). The activity of the bioanode fabric was enhanced by optimizing the buffer concentration to 0.5 M (red bold line). (b) Current density at 0.6 V vs. Ag/AgCl of the FDH anode measured in different buffer concentration. The measurements were carried out for the same FDH anode specimen. (For interpretation of the references to color in this figure legend, the reader is referred to the web version of this article.)

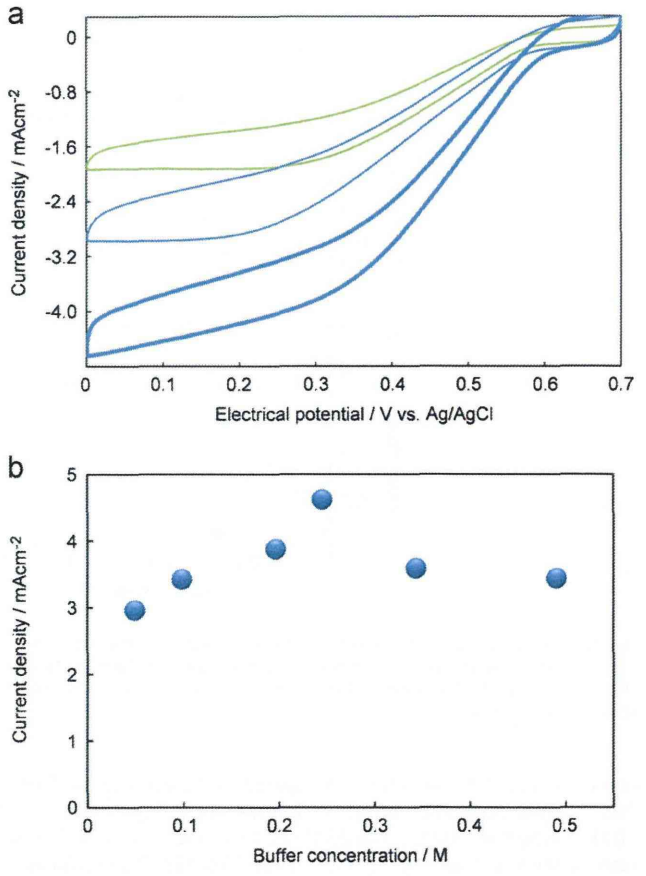

Fig. 3. (a) Cyclic voltammograms of O_2 reduction at a BOD/CNT-modified CF strip measured at 10 mV s^{-1} on the solution (green). The activity of the CF electrode was enhanced by further modification with CNT after the BOD immobilization (blue line) and by subsequent optimization of buffer concentration (bold blue). (b) Current density at 0 V vs. Ag/AgCl of the BOD cathode fabric with different buffer concentration. (For interpretation of the references to color in this figure legend, the reader is referred to the web version of this article.)

performance was drastically enhanced by increasing the buffer concentration in the measurement solutions from 50 mM to 0.5 M (red bold line). This is made possible by the existence of adequate buffer capacities that prevent local pH changes caused by oxidation products. Excess buffer concentration, however, lead to a low current density (see Fig. 2b). This is probably due to lowering of the enzyme activity because the enzyme is exposed by a high ionic strength solution. The maximum current of the optimized bioanode produced 15.8 mA (28.0 mA cm^{-2}) at 0.6 V using a 500 mM buffer. Even in quiescent conditions, the current reached 5.8 mA (10 mA cm^{-2}) at 0.6 V (Supplementary Fig. 2), being equivalent to that in DN hydrogel made with 500 mM McIlvaine buffer solution (pH 5.0) containing 500 mM fructose.

3.2. Performance of gas-diffusion biocathodes

Fig. 3a shows cyclic voltammograms of a BOD-modified CF cathode at 10 mV s^{-1}. The electrode strip was put on an oxygenic pH 5.0 buffer solution so as to contact the solution by the BOD-modified face (green line). The reduction current density reaches ~1.9 mA cm^{-2} (at 0 V) by utilizing an oxygen supply from the ambient air through the CF. Moreover, an additional CNT coating onto the BOD-modified face of the CF strip enhanced the performance further to 2.9 mA cm^{-2}. Presumably, the hydrophobic nature of that coating controls excess penetration of solution into the CF electrodes (Supplementary Fig. 3) (Miyake et al., 2011b; Haneda et al., in press). In addition to optimizing the performance of the bioanode fabric, the cathodic performance can be optimized by changing the buffer concentration (Fig. 3b); the maximum current was 4.6 mA cm^{-2} at 0 V using a 250 mM buffer condition.

3.3. Performance of the laminated biofuel cell sheets

The FDH/CNT-modified CF anode and the CNT/BOD/CNT-modified gas-diffusion CF cathode were laminated to the opposite faces of a DN hydrogel sheet (0.5 mm thick) made with 250 mM McIlvaine buffer solution (pH 5.0) containing 500 mM fructose. The enzyme-modified hydrophilic anode appeared to become moistened by blotting of the solution from the hydrogel layer. On the other hand, the O_2 reduction at the hydrophobic cathode proceeded at the three-phase boundary of the hydrogel–electrode interface. Fig. 4a shows typical examples of the cell performance. The open-circuit voltage of the cell was 0.74 V, which is similar to the difference between the potentials at which fructose oxidation and oxygen reduction start to occur in cyclic voltammograms (−0.14 V and 0.60 V in Figs. 2a and 3, respectively). The maximum power density reached 0.95 mW cm^{-2} at 0.36 V, which was determined by the BOD-cathode fabric because of its

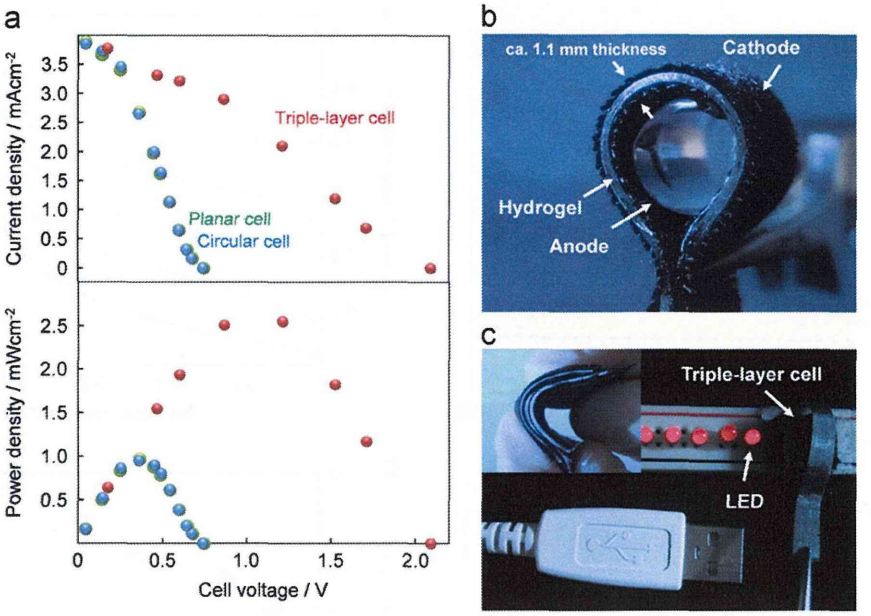

Fig. 4. (a) Performance of the biofuel cell (1 cm × 0.2 cm × 1.1 mm) with and without bending. The internal hydrogel layer was made with 250 mM McIlvaine buffer solution (pH 5.0) containing 500 mM fructose. The performance of a triple-layer cell is also shown. (b) Photograph of the biofuel cell sheet bend into a circle. (c) Photograph of the emission from LEDs connected with the triple-layer cell (inset). (For interpretation of the references to color in this figure legend, the reader is referred to the web version of this article.)

comparatively inferior activity compared to the FDH-anode fabric. The internal resistance of the cells was negligibly small, being 10 Ω hydrogel resistance and 26 Ω cell resistance measured by AC impedance spectroscopy (± 5 mV, 1–10,0000 Hz). The stability of the cells decreased extremely for few hours. Since the bioelectrodes maintained 85% performance in 500 mM fructose buffer solution (pH 5.0) for 24 h (Supporting Fig. 4), the shorter stability is due to drying of the hydrogel.

Importantly, the performance of the cell bent into an circle (blue plots) is almost identical to that of a cell that was not bent (green plots). Such high flexibility originates in the superior mechanical strength of both the fabric bioelectrodes and the DN hydrogel. As shown in Fig. 4b, the present laminar cell is thin, being only 1.12 mm thick, which also leads to a flexible character. Moreover, owing to the characteristic properties of the hydrogel, the laminar cell requires no sealing frame. Such important cell characteristics confer attractive advantage from a practical viewpoint. The application of such a laminar cell for boosting the output voltage is demonstrated in Fig. 4. The booster cell was fabricated simply by lamination of anode/hydrogel/cathode sheets (see Fig. 1d). As shown in Fig. 4a (red plots), the open-circuit voltage of the laminated cell was 2.09 V, which is 2.8-fold that of a single cell. The maximum current was quite similar to that of the single cell. These results indicate that layered cells can be connected in series without suffering from short-circuit, even without packaging. Ionic isolation between the cells could be avoided by the hydrophobicity of gas-diffusion cathodes and the solid-like property of hydrogels. The laminated cell produced a maximum power of 0.64 mW at 1.21 V (2.55 mW cm^{-2}, 6.28 mW cm^{-3}); using this level of power, we were able to light the LEDs, as demonstrated in Fig. 4c.

4. Conclusions

We have developed layered biofuel cells constructed by laminating FDH/CNT-modified CF strips, fuel-containing DN hydrogel films, and CNT/BOD/CNT-modified gas-diffusion CF strips. A single-layer cell of anode/hydrogel/cathode sheets was very thin (1.1 mm thickness), and exhibited high flexibility, being resistant to a circular bending stress. A triple-layer cell produced a higher open circuit voltage of 2.09 V corresponding to a 2.8-fold improvement over the single cell voltage (0.74 V) and a maximum power of 0.64 mW (2.55 mW cm^{-2}) at 1.21 V, indicating a successful series-connection even without packaging of each cell. It is important to note that the output voltage can easily be tuned by changing the number of layers. Such a flexible, tunable, totally organic power source could be combined in the future with wearable electronics.

Acknowlegement

The carbon fabric and carbon nanotubes were kindly donated from Toho Tenax Co. and Bayer Co., respectively. This work was partly supported by the Noguchi Institute.

Appendix A. Supporting information

Supplementary data associated with this article can be found in the online version at http://dx.doi.org/10.1016/j.bios.2012.05.041.

References

Barton, S.C., Gallaway, J., Atanassov, P., 2004. Chemical Reviews 104 (10), 86–4867.
Cooney, M.J., Svoboda, V., Lau, C., Martin, G., Minteer, S.D., 2008. Energy and Environmental Science 1 (3), 320–337.
Ferrigno, R., Stroock, A.D., Clark, T.D., Mayer, M., Whitesides, G.M., 2002. Journal of the American Chemical Society 124 (44), 12930–12931.
Gao, F., Viry, L., Maugey, M., Poulin, P., Mano, N., 2010. Nature Communications 1, 2.
Gellett, W., Kesmez, M., Schumacher, J., Akers, N., Minteer, S.D., 2010. Electroanalysis 7, 727–731.
Gong, J.P., 2010. Soft Matter. 6 (12), 2583–2590.

Haneda, K., Yoshino, S., Ofuji, T., Miyake, T., Nishizawa, M. Electrochimica Acta 1–4, in press. http://dx.doi.org/10.1016/j.electacta.2012.01.112.
Heller, A., 2004. Physical Chemistry Chemical Physics 6 (2), 209–216.
Holzinger, M., Le Goff, A., Cosnier, S. Electrochimica Acta, in press. http://dx.doi.org/10.1016/j.electacta.2011.12.135.
Miyake, T., Yoshino, S., Yamada, T., Hata, K., Nishizawa, M., 2011a. Journal of the American Chemical Society 133 (13), 5129–5134.
Miyake, T., Haneda, K., Nagai, N., Yatagawa, Y., Onami, H., Yoshino, S., Abe, T., Nishizawa, M., 2011b. Energy & Environmental Science 4, 5008–5012.
Murata, K., Kajiya, K., Nakamura, N., Ohno, H., 2009. Energy & Environmental Science 2 (12), 1280–1285.
Sakai, H., Nakagawa, T., Tokita, Y., Hatazawa, T., Ikeda, T., Tsujimura, S., Kano, K., 2009. Energy & Environmental Science 2 (1), 133–138.
Tominaga, M., Shirakihara, C., Taniguchi, I., 2007. Journal of Electroanalytical Chemistry 610 (1), 1–8.
Tominaga, M., Nomura, S., Taniguchi, I., 2009. Biosensors & bioelectronics 24 (5), 1184–1188.
Tsujimura, S., Kamitaka, Y., Kano, K., 2007. Fuel Cells 7 (6), 463–469.
Tsujimura, S., Nishina, A., Hamano, Y., Kano, K., Shiraishi, S., 2010. Electrochemistry Communications 12 (3), 446–449.
Wen, D., Xu, X., Dong, S., 2011. Energy & Environmental Science 4 (4), 1358–1363.
Willner, I., Yan, Y.-M., Willner, B., Tel-Vered, R., 2009. Fuel Cells 9 (1), 7–24.
Wu, Z.L., Gong, J.P., 2011. NPG Asia Materials 3 (6), 57–64.
Zebda, A., Gondran, C., Le Goff, A., Holzinger, M., Cinquin, P., Cosnier, S., 2011. Nature Communications 2, 370.

ADVANCED ENERGY MATERIALS
www.advenergymat.de

Materials Views
www.MaterialsViews.com

Molecularly Ordered Bioelectrocatalytic Composite Inside a Film of Aligned Carbon Nanotubes

*Syuhei Yoshino, Takeo Miyake, Takeo Yamada, Kenji Hata, and Matsuhiko Nishizawa**

Molecularly ordered composites of polyvinylimidazole-[Os(bipyridine)$_2$Cl] (PVI-[Os(bpy)$_2$Cl]) and glucose oxidase (GOD) are assembled inside a film of aligned carbon nanotubes. The structure of the prepared GOD/PVI-[Os(bpy)$_2$Cl]/CNT composite film is entirely uniform and stable; more than 90% bioelectrocatalytic activity could be maintained even after storage for 6 d. Owing to the ideal positional relationship achieved between enzyme, mediator, and electrode, the prepared film shows a high bioelectrocatalytic activity for glucose oxidation (ca. 15 mA cm^{-2} at 25 °C) with an extremely high electron-transfer turnover rate (ca. 650 s^{-1}) comparable to the value for GOD solutions, indicating almost every enzyme molecule entrapped within the ensemble (ca. 3×10^{12} enzymes in a 1 mm × 1 mm film) can work to the fullest extent. This free-standing, flexible composite film can be used by winding on a needle device; as an example, a self-powered sugar monitor is demonstrated.

1. Introduction

Controlling the electrical contact of redox enzymes with electrodes is a critical issue for enzymatic biodevices such as biofuel cells and biosensors.[1–12] The mutual positioning between enzyme molecules, mediator molecules (not always necessary), and electrode surface determines the efficiency, reproducibility, and stability of the bioelectrocatalysis systems. A conventional engineering for accelerating the electron transfer to the redox enzymes is inclusive immobilization with mediator polymer matrices, in which the successive electron exchange between the neighboring mediator groups connects the enzyme redox center and the electrode surface.[10–12] For example, Os-complex-pendant polymers are successful mediating matrices for glucose oxidase (GOD) and can provide glucose oxidation current at a mA cm^{-2} level.[13–16] Barton et al. reported ca. 20 mA cm^{-2} using GOD, an Os-complex polymer, and a carbon nanotube (CNT)-modified electrode.[16] However, because of random mutual positioning in the 3D composite, many enzyme molecules are isolated from the molecular network for continuous bioelectrocatalysis. On the other hand, direct immobilization of an enzyme monolayer on the electrode surface has improved the efficiency of enzyme utilization. A striking example is the reconstituting apo-GOD on a relay-FAD monolayer linked to electrode surfaces.[2,17–20] Since all the enzyme units are oriented in an optimal position with respect to the electrode surface, a high electron-transfer turnover rate comparable to that for bulk GOD reaction (approximately 700 s^{-1} at 25 °C) has been achieved. However, the drawback of such 2D monolayer engineering is the lower bioelectrocatalytic performance due to the limited amount of immobilized enzymes.

We present herein an enzyme/mediator/electrode ordered ensemble that shows both "high turnover rate" and "large catalytic current". In order to satisfy both of these requirements, the larger amount of enzymes than monolayer should be immobilized while keeping effective contact with electrodes. We realize such ideal conditions by taking advantage of a film of well-aligned carbon nanotube forest (CNTF)[21] consisting of single-walled CNTs arrayed with a pitch of 16 nm. The CNTF was synthesized by water-assisted chemical vapor deposition on a line-patterned Al_2O_3/Fe catalyst on silicon wafers (see the Experimental Section for details).[21] As shown in **Figure 1**a, the synthesized CNTF film (1.5 mm × 1 mm) was pulled from the substrate and pinched by inverse operating tweezers (electrical lead), to produce an exposed electrode geometric area of ca. 2 mm^2 (sum of both faces of a 1 mm × 1 mm sheet). The thickness of the CNTF films (4, 12, or 20μm) was determined by the width of the line-patterns of Al_2O_3/ Fe catalyst. Recently, we reported that the intraspace of the CNTF is useful for immobilization of fructose dehydrogenase and laccase, which are the direct electron transfer (DET)-type enzymes.[22] Although there are a few recent reports that also GOD is capable of direct communication with electrodes,[23–25] our repeated attempts to prepare a workable GOD/CNTF ensemble electrode without any mediators have failed. Therefore we developed a stepwise process to construct the molecular architecture with polyvinylimidazole-[Os(bipyridine)$_2$Cl] (PVI-[Os(bpy)$_2$Cl]; MW: 15 000) and GOD (EC:1.1.3.4; MW: 186 kDa), as illustrated in Figure 1b and 1c. The PVI-[Os(bpy)$_2$Cl] was synthesized according to a

S. Yoshino, Dr. T. Miyake, Prof. M. Nishizawa
Department of Bioengineering and Robotics
Tohoku University
6-6-1 Aoba, Sendai 980-8579, Japan
E-mail: nishizawa@biomems.mech.tohoku.ac.jp
Dr. T. Yamada, Dr. K. Hata
National Institute of Advanced Industrial Science and Technology (AIST)
Tsukuba Central 5, 1-1-1 Higashi, Tsukuba, Ibaraki 308-8565, Japan
Dr. T. Miyake, Dr. T. Yamada, Dr. K. Hata, Prof. M. Nishizawa
Core Research for Evolutional Science and Technology (CREST)
Japan Science and Technology Agency (JST)
Tokyo 102-0075, Japan

DOI: 10.1002/aenm.201200422

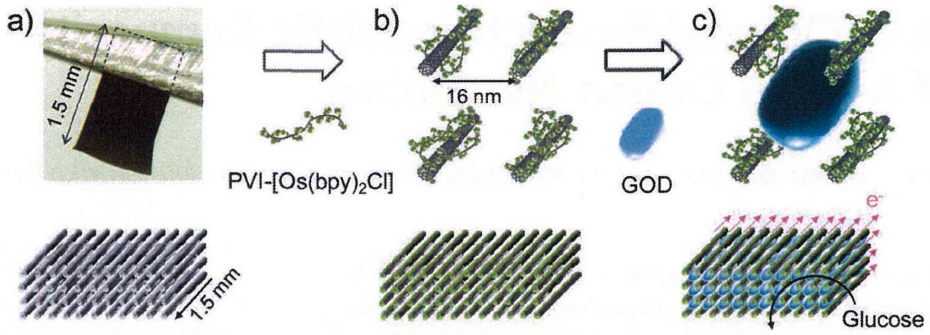

Figure 1. Schematic illustration of the stepwise process for constructing bioelectrocatalytic composite inside a CNTF film.

literature method,[26] with a molar ratio of imidazole group to $[Os(bpy)_2Cl]$ of 5.

2. Results and Discusssion

2.1. Adsorption of PVI-$[Os(bpy)_2Cl]$ inside CNTF Films

The CNTF film was first treated with 0.1% Triton X-100 to make it hydrophilic, and then soaked in a stirred phosphate buffer solution (PBS, pH 7.0) containing 1 mg mL^{-1} PVI-$[Os(bpy)_2Cl]$ at 4 °C. As shown in **Figure 2**a, the cyclic voltammogram (CV) of the treated CNTF showed a symmetric shape typical for adsorbed redox species.[27] In fact, the amplitude of peak currents were proportional to the scan rates (Figure 2b). The amount of PVI-$[Os(bpy)_2Cl]$ adsorbed within the CNTF films were estimated by integrating the CV currents and is plotted in Figure 2c against the soaking time in the 1 mg mL^{-1} PVI-$[Os(bpy)_2Cl]$ solution. The amount of PVI-$[Os(bpy)_2Cl]$ in a CNTF film increased with the soaking time and reached a maximum after 2 h. Importantly, these values are proportional to the CNTF film thickness (7.2×10^{-10} mol for a 12 μm thick film and 12.8×10^{-10} mol for a 20 μm thick film), indicating that the PVI-$[Os(bpy)_2Cl]$ molecules can entirely and uniformly adsorbed inside the CNTF films, as illustrated in Figure 1b. A part of the free imidazole groups of the mediator polymer would adsorb on CNT surfaces via π–π interaction.[28] The adsorption density of PVI-$[Os(bpy)_2Cl]$ calculated using the effective inner surface area of the CNTF films ($8.2\ cm^2$ for 20 μm thick film)[21] was $(1.6 \pm 0.1) \times 10^{-10}$ mol cm^{-2}, which is comparable with the value for a PVI-$[Os(bpy)_2Cl]$ film adsorbed on a flat Au surface (3.2×10^{-10} mol cm^{-2}).[29]

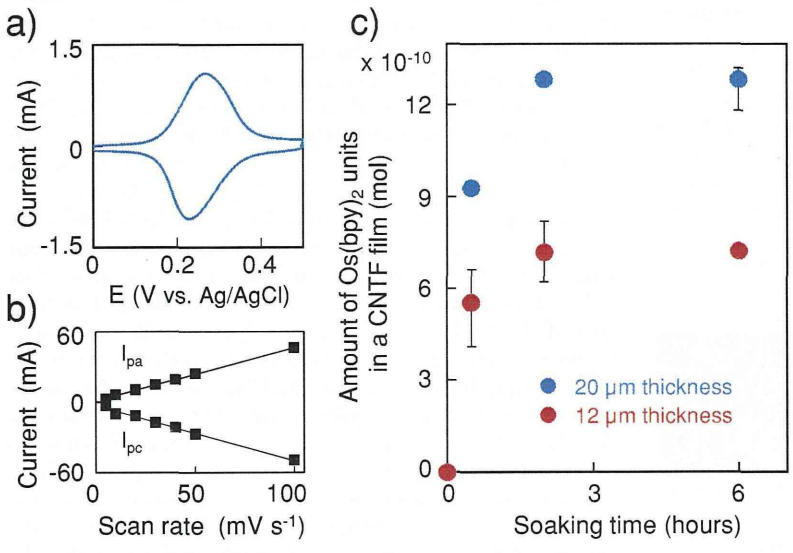

Figure 2. a) Cyclic voltammograms at 10 mV s^{-1} of the PVI-$[Os(bpy)_2Cl]$-modified CNTF film (20 μm thickness) in PBS (pH 7.0). A CNTF film was soaked in the 1 mg mL^{-1} PVI-$[Os(bpy)_2Cl]$ PBS for 6 h. b) Redox peak currents of the CVs as a function of scan rate. c) The amount of $Os(bpy)_2$ unit inside a CNTF film (film thickness: 12 and 20 μm) as a function of soaking time for 1 mg mL^{-1} PVI-$[Os(bpy)_2Cl]$ PBS solution. The mean values (± standard deviation) of three independent specimens are given.

2.2. Electrocatalytic Activity of GOD/PVI-$[Os(bpy)_2Cl]$/CNTF Ensemble Films

Subsequent loading of the enzyme GOD was conducted by immersing the PVI-$[Os(bpy)_2Cl]$-adsorbed CNTF films in a stirred PBS solution (pH 7.0) containing 3 mg ml^{-1} GOD for 1 hour. **Figure 3**a shows the CVs of GOD/PVI-$[Os(bpy)_2Cl]$/CNTF ensemble films at 10 mV s^{-1} in a stirred 200 mM-glucose PBS solution. The catalytic current for glucose oxidation increased in response to the thickness of CNTF films (3.7 mA cm^{-2} for 4 μm thickness and 14.7 mA cm^{-2} for 20 μm thickness), indicating that also GOD can entirely penetrate inside the PVI-$[Os(bpy)_2Cl]$-modified CNTF films. For example, the content of GOD incorporated in a 20 μm thick film was measured as ca. 0.86 μg by a C-6667 Protein Quantitation Kit, the value being a little below the case when GOD molecules ($6.7 \times 6.7 \times 21\ nm^3$)[30] align to form lines in the interspace of CNTs (1.17 μg). The current density under stirred condition was enhanced to as high as 26.7 mA cm^{-2} by turning up the buffer temperature to 37.5 °C. This glucose

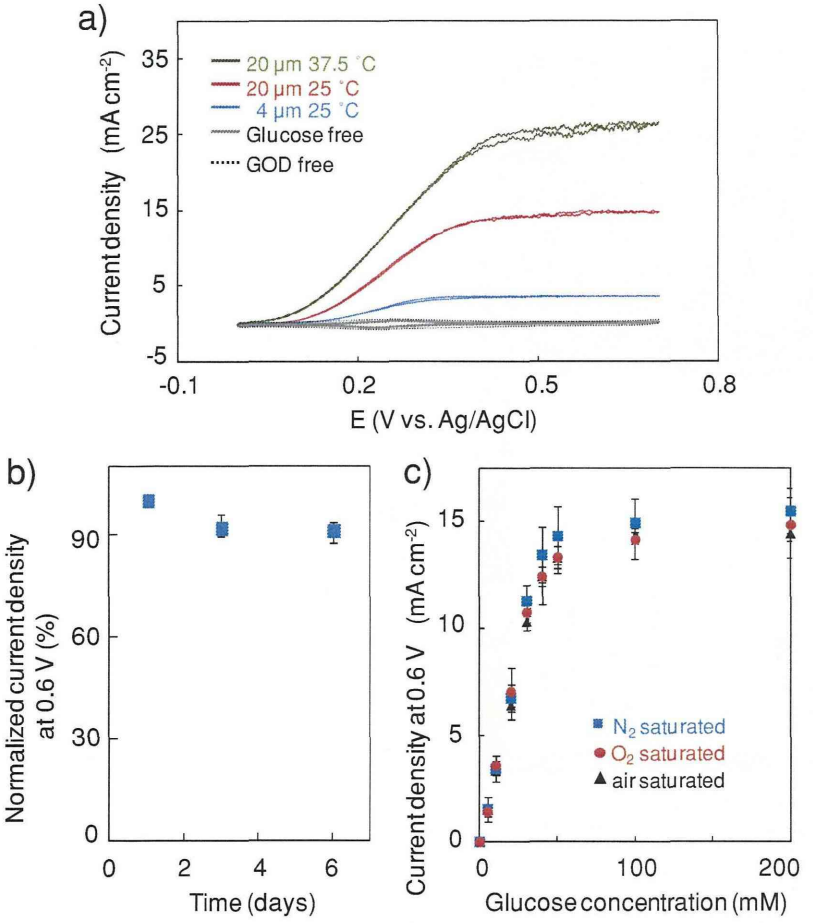

Figure 3. a) Cyclic voltammograms of GOD/PVI-Os/CNTF ensemble films at 10 mV s^{-1} in stirred air-saturated 25 °C (or 37.5 °C) PBS containing 200 mM-glucose. The thicknesses of CNTF films were 4 or 20 µm. The control voltammograms without GOD and glucose are also shown. We used a total geometric area of the pinched film (2 mm^2) for the calculation of the current densities. b) The oxidation current densities at 0.6 V vs. Ag/AgCl for the GOD/PVI-[$Os(bby)_2Cl$]/CNTF film (20 µm thickness) in a stirred 200 mM-glucose PBS solution, periodically measured during 6 d of storage in PBS solution. c) The current densities at 0.6 V for the 20 µm GOD/PVI-[$Os(bby)_2Cl$]/CNTF film as a function of the glucose concentration, measured in O_2-, N_2-, and air-saturated stirred PBS (pH 7.0) solutions. The mean values (± standard deviation) of three independent specimens are given.

oxidation activity is comparable or superior to those previously reported using GOD.[13–16] In a quiescent condition, the current density decreased by half, probably due to the limited mass-transfer inside the film. Importantly, more than 90% of the electrode activity could be maintained even after 6 d storage in an air-saturated PBS solution (Figure 3b), proving the stability of bioelectrocatalytic architecture with the composite of PVI-[$Os(bpy)_2Cl$] polymer and GOD. The anionic GOD molecules could be stably entrapped by electrostatic interaction with cationic Os-complex of the mediator polymer that is anchored on the CNT surface via π–π interaction.[28]

The electron-transfer turnover rate for the 20 µm thick film was calculated from the current value at 25 °C (0.29 mA), the Faraday constant (96 500 C mol^{-1}), the molecular weight of GOD (186 000 g mol^{-1}), and the content of GOD molecules in a piece of the ensemble film (ca. 0.86 µg). The derived averaged turnover rate was ca. 650 s^{-1}, being comparable to that of GOD in bulk solution containing the natural electron acceptor O_2 (700 s^{-1}) at 25 °C.[31] These results indicate that most of ca. 3×10^{12} GOD units within the film could efficiently work to the fullest extent, presumably owing to the molecularly ordered structure of enzyme/mediator/electrode ensemble. Such a high efficiency of the present GOD electrode resulted in a resistance to oxygen inhibition, as shown in Figure 3c. The catalytic performance was almost identical in N_2-saturated, air-saturated, and even O_2-saturated solutions. In general, glucose oxidation with GOD-modified electrodes is often disturbed by dissolved O_2, which is troublesome for glucose sensing.[32,33] However, the ordered $Os(bby)_2$ groups in the present ensemble electrode could effectively accept the electron from GOD in preference to O_2, resulted in excellent O_2 resistance.

2.3. Application as a Flexible Anode of Biofuel Cells

The present free-standing, bioelectrocatalytic film could be used for miniature biofuel cell devices. We demonstrate here the application of the film to a self-powered sugar indicator designed for inserting into a fruit. For indicating the glucose concentration, the net performance of the biofuel cell system should be controlled by the glucose anode. Because the oxygen in fruits is limited to a lower concentration than glucose, we employ a gas-diffusion biocathode[34] for utilizing the abundant oxygen in air outside of the fruits (see the Experimental Section for details). **Figure 4**a shows the biofuel cell performance measured using 200 mM glucose PBS solution with a couple consisting of a GOD/PVI-[$Os(bby)_2Cl$]/CNTF film anode (20 µm thickness) and a cathode made from bilirubin oxidase (BOD)-modified carbon fabric (1 cm × 1 cm). The open-circuit voltage of the cell was 0.5 V in agreement with the difference between the potentials at which glucose oxidation and oxygen reduction start to occur in cyclic voltammetry (0.1 V in Figure 3a and 0.6 V in Figure S1, see the Supporting Information). The maximum output current (0.27 mA) is almost equivalent to the maximum oxidation current at the composite anode (0.29 mA) that can be calculated by the current density in Figure 3a (14.7 mA cm^{-2}) and the electrode area of 2 mm^2. This result indicates that the system is limited by the anode even in 200 mM glucose, a concentration that is markedly higher than that found in raw fruits (a few tens of mM). As shown in Figure 4b, a piece of GOD/PVI-[$Os(bby)_2Cl$]/CNTF film was wound on one lead of a light-emitting-diode (LED) device, whose blinking interval is inversely proportional

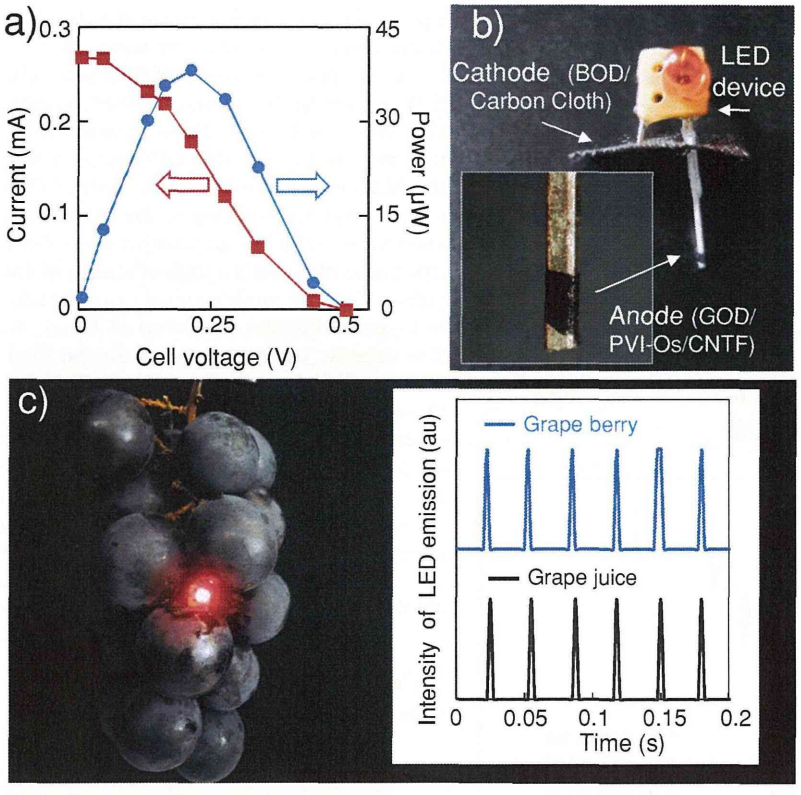

Figure 4. a) Performance of a biofuel cell composed of an anode of GOD/PVI-[Os(bby)$_2$Cl]/CNTF film (20 μm thickness) and a cathode of BOD-modified carbon cloth (1 cm × 1 cm) in 200 mM glucose PBS solution, measured by changing the external resistance (28 to 46kΩ). b) Photograph of the LED-based self-powered sugar indicator, at the tip of which the GOD/PVI-[Os(bby)$_2$Cl]/CNTF film was wound. c) The device assembly was inserted in a grape and the LED blinking was measured (inset). The time course of LED emission, taken using an extracted juice, is also shown.

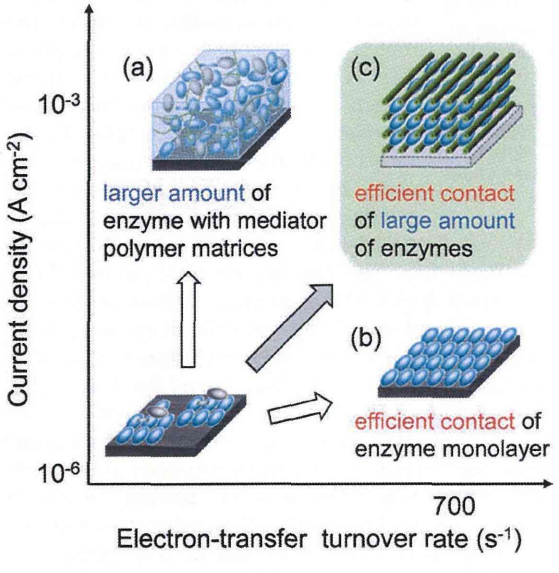

Figure 5. Scheme showing correlative characters of: a) an enzyme-film with mediator polymer matrices for larger current, b) an enzyme-monolayer electrode for higher turnover rate, and, c) the present ensemble electrode for both large current and high turnover rate.

to the power of the biofuel cell.[35,36] The other lead was connected to the BOD-based gas-diffusion cathode. The blinking interval of the LED upon inserting the device to a grape was coincident with that for the extracted juice (Figure 4c), proving that this device could serve as a sugar indicator by simply being inserted into a grape. We confirmed that there is no corrosion reaction at the LED lead wire during the operation. The present principle of the self-powered sensor could be applied to more important blood sugar monitoring applications; we are planning to develop a GOD/PVI-[Os(bby)$_2$Cl]/CNTF-based device structure suitable for low-invasive insertion into a blood vessel through skins.

3. Conclusions

An amount of enzyme units larger than that in a monolayer were successfully immobilized while keeping effective electrical contact with the electrode (CNTs), as summarized in **Figure 5**. In particular, we have succeeded in forming an entirely uniform bioelectrocatalytic architecture with PVI-[Os(bby)$_2$Cl] and GOD inside a CNTF film. The voltammograms of the PVI-[Os(bby)$_2$Cl]-modified CNTF indicated the uniform adsorption of PVI-[Os(bpy)$_2$Cl] on the CNT surface via π–π interaction with the density of ca. $(1.6 \pm 0.1) \times 10^{-10}$ mol cm^{-2}. The subsequent GOD seemed to become stably entrapped at the interspaces of PVI-[Os(bby)$_2$Cl]-modified CNTs by the electrostatic interaction. Owing to the ordered positional relationship between GOD, PVI-[Os(bby)$_2$Cl], and CNT, the composite film showed both high activity for glucose oxidation (ca. 15 mA cm^{-2}) and high electron-transfer turnover rate (ca. 650 s^{-1}), indicating almost every enzyme molecules within the film could work to the fullest extent.

4. Experimental Section

CNTF Preparation: CNTF was synthesized in a 1 inch tube furnace by water-assisted chemical vapor deposition at 750 °C with a C_2H_4 carbon source and an Al_2O_3 (10 nm)/Fe (1.0 nm) thin-film catalyst grown on silicon wafers.[21] We used He with H_2 as the carrier gas (total flow 1000 standard cubic centimeters per minute (sccm)) at 1 atm with a controlled amount of water vapor with ethylene (100 sccm) for 10 min.

Quantitative Analysis of the Entrapped Enzymes: The quantitative analysis of GOD was conducted as explained in our previous paper.[22] The enzyme-incorporated CNTF film was first washed and immersed in 20 mM sodium phosphate buffer (pH 9.3) containing 0.1 M sodium borate and 1% sodium cholate and dispersed with an ultrasonic homogenizer for 15 min. The GOD in the dispersion was then analyzed using a C-6667 Protein Quantitation Kit (Molecular Probes), using 5 mM (3-(4-carboxybenzoyl)-quinoline-2-carboxaldehyde) (ATTO-TAG CBQCA) and 20 mM KCN to label the enzyme with CBQCA. After 1.5 h of incubation, the fluorescent intensity was measured by a luminescent

image analyzer system (Fuji Photo Film, LAS-3000 mini), and the amount of enzyme was determined by referencing a calibration curve.

Preparation of Gas-diffusion Carbon Fabric (CF) Cathodes: The preparation of the cathode basically followed the procedures used for our previous work.[34] A 40 μL aliquot of a 10 mg mL^{-1} multiwalled CNT solution was put on a CF strip and dried in air, followed by thoroughly washing out the surfactant by soaking in an ethanol solution for more than 1 h with stirring. The surface of the CNT-modified CF electrode was further modified with a 0.1 mL solution of 5 mg mL^{-1} bilirubin oxidase (BOD, EC 1.3.3.5, 2.5 U mg^{-1}, from Myrothecium) in a vacuum oven (0.09 MPa, 35 °C). The strip was additionally coated with the CNT solution to make the surface hydrophobic.

Electrochemical Measurements: The GOD/PVI-[Os(bpy)$_2$Cl]/CNTF ensemble films, anchored at the edge with SUS316L fine tweezers, was analyzed by a three-electrode system (BSA, 730C electrochemical analyzer) in stirred solutions using a Ag/AgCl reference and a platinum counter electrode. The gas-diffusion cathode (BOD-modified CF strip) was put on an air-saturated solution so as to contact the solution by the BOD-modified face during cyclic voltammetry (Figure S1 in the Supporting Information). The performance of a biofuel cell constructed from an GOD-based CNTF anode and an BOD-based CF cathode was evaluated on the basis of the cell voltage upon changing the external resistance between 1 kΩ and 2 MΩ at the time step of 60 s. Unless otherwise indicated, the electrochemical measurements were carried out at room temperature (25 °C).

Supporting Information

Supporting Information is available from the Wiley Online Library or from the author.

Acknowledgements

Authors express appreciation to Toho Tenax Co. for donation of the carbon fabrics and to Bayer Co. for multiwalled carbon nanotubes.

Received: June 8, 2012
Revised: June 29, 2012
Published online: August 24, 2012

[1] I. Willner, Z. Katz, *Bioelectronics*, Wiley-VCH,Weinheim Germany **2005.**
[2] I. Willner, Y. M. Yan, B. Willner, R. Tel-Vered, *Fuel Cells* **2009**, *1*, 7.
[3] G. T. R. Palmore, H. Bertschy, S. H. Bergens, G. M. Whitesides, *J. Electroanal. Chem.* **1998**, *443*, 155.
[4] R. L. Arechederra, S. D. Minteer, *Fuel Cells* **2009**, *1*, 63.
[5] W. Gellett, M Kesmez, J. Schumacher, N. Akers, S. D. Minteer, *Electroanalysis* **2010**, *22*, 727.
[6] S. D. Minteer, P. Atanassov, H. R. Luckarift, G. R. Johnson, *Mater. Today* **2012**, *15*, 166.
[7] L. Halámková, J. Halámek, V. Bocharova, A. Szczupak, L. Alfonta, E. Katz, *J. Am. Chem. Soc.* **2012**, *134*, 5040.
[8] D. Leecha, P. Kavanagha, W. Schuhmann, *Electrochim. Acta* **2012**, DOI:10.1016/j.electacta.2012.02.087.
[9] M. Holzinger, A. L. Goff, S. Cosnier, *Electrochim. Acta* **2012**, DOI:10.1016/j.electacta.2011.12.135.
[10] A. Heller, B. Feldman, *Acc. Chem. Res.* **2010**, *43*, 963.
[11] S. G. Barton, J. Gallaway, P. Atanassov, *Chem. Rev.* **2004**, *104*, 4867.
[12] W. Schuhmann, T. J. Ohara, H. L. Schmidt, A. Heller, *J. Am. Chem. Soc.* **1991**, *113*, 1394.
[13] F. Mao, N. Mano, A. Heller, *J. Am. Chem. Soc.* **2003**, *125*, 4951.
[14] F. Gao, L. Viry, M. Maugey, P. Poulin, N. Mano, *Nat. Commun.* **2010**, *1*, 2.
[15] H. Wen, V. Nallathambi, D. Chakraborty, S. C. Barton, *Microchim. Acta* **2011**, *175*, 283.
[16] S. C. Barton, Y. Sun, B. Chandra, S. White, J. Hone, *Electrochem. Solid-State Lett.* **2007**, *10*, B96.
[17] Y. Xiao, F. Patolsky, E. Katz, J. F. Hainfeld, I. Willner, *Science* **2003**, *299*, 1877.
[18] F. Patolsky, Y. Weizmann, I. Willner, *Angew. Chem., Int. Ed.* **2004**, *43*, 2113.
[19] M. Zayats, E. Katz, I. Willner, *J. Am. Chem. Soc.* **2002**, *124*, 2120.
[20] I. Willner, V. Heleg-Shabtai, R. Blonder, E. Katz, G. Tao, A.F. Bückmann, A. Heller, *J. Am. Chem. Soc.* **1996**, *118*, 10321.
[21] D. N. Futaba, K. Hata, T. Yamada, T. Hiraoka, Y. Hayamizu, Y. Kakudate, O. Tanaike, H. Hatori, M. Yumura, S. Iijima, *Nat. Mater.* **2006**, *5*, 987.
[22] T. Miyake, S. Yoshino, T. Yamada, K. Hata, M. Nishizawa, *J. Am. Chem. Soc.* **2011**, *133*, 5129.
[23] A. Guiseppi-Elie, C. Lei, R. H. Baughman, *Nanotechnology* **2002**, *13*, 559.
[24] A. Zebda, C. Gondran, A. L. Goff, M. Holzinger, P. Cinquin, S. Cosnier, *Nat. Commun.* **2011**, *2*, 1.
[25] J. T. Holland, C. Lau, S. Brozik, P. Atanassov, S. J. Banta, J. *Am. Chem. Soc.* **2011**, *133*, 19262.
[26] T. J. Ohara, R. Rajagopalan, A. Heller, *Anal. Chem.* **1993**, *65*, 3512.
[27] A. J. Bard, L. R. Faulkner, *Electrochemical Methods: Fundamental and Applications*, Wiley, New York, 2001, 589.
[28] T. Roman, W. A. Dino, H. Nakanish, H. Kasai, *Eur. Phys. J. D* **2006**, *38*, 117.
[29] Y. Wang, P. P. Joshi, K. L. Hobbs, M. B. Johnson, D. W. Schmidtke, *Langmuir* **2006**, *22*, 9776.
[30] G. Wohlfahrt, S. Witt, J. Hendle, D. Schomburg, H. M. Kalisz, H. Hecht, *J. Acta Cryst., Sect. D: Biol. Crystallogr.* **1999**, *D55*, 969.
[31] C. Bourdillon, C. Demaille, J. Gueris, J. Moiroux, J. M. Savebant, *J. Am. Chem. Soc.* **1993**, *115*, 12264.
[32] J. Wang, *Electroanalysis* **2001**, *13*, 983.
[33] B. A. Gregg, A. Heller, *Anal. Chem.* **1990**, *62*, 258.
[34] K. Haneda, S. Yoshino, T. Ofuji1, T. Miyake, M. Nishizawa, *Electrochim. Acta* **2012**, DOI: 10.1016/j.electacta.2012.01.112.
[35] T. Hanashi, T. Yamazaki, W. Tsugawa, S. Ferri, D. Nakayama, M. Tomiyama, K. Ikebukuro, K. Sode, *Biosens. Bioelectron.* **2009**, *24*, 1837.
[36] T. Miyake, K. Haneda, N. Nagai, Y. Yatagawa, H. Onami, S. Yoshino, T. Abe, M. Nishizawa, *Energy Environ. Sci.* **2011**, *4*, 5008.

Spatiotemporally controlled contraction of micropatterned skeletal muscle cells on a hydrogel sheet†

Kuniaki Nagamine,[ab] Takeaki Kawashima,[a] Soichiro Sekine,[a] Yuichiro Ido,[a] Makoto Kanzaki[bc] and Matsuhiko Nishizawa*[ab]

Received 1st September 2010, Accepted 3rd November 2010
DOI: 10.1039/c0lc00364f

We have developed gel sheet-supported C_2C_{12} myotube micropatterns and combined them with a microelectrode array chip to afford a skeletal muscle cell-based bioassay system. Myotube line patterns cultured on a glass substrate were transferred with 100% efficiency to the surface of fibrin gel sheets. The contractile behavior of each myotube line pattern on the gel was individually controlled by localized electrical stimulation using microelectrode arrays that had been previously modified with electropolymerized poly(3,4-ethylenedioxythiophene) (PEDOT). We successfully demonstrated fluorescent imaging of the contraction-induced translocation of the glucose transporter, GLUT4, from intracellular vesicles to the plasma membrane of the myotubes. This device is applicable for the bioassay of contraction-induced metabolic alterations in a skeletal muscle cell.

Introduction

In vitro bioassay systems incorporating cells with physiological activity have been developed as an alternative to whole animal experiments.[1,2] Systems using skeletal muscle cells are one of the promising devices to reveal the complex mechanisms of type 2 diabetes because that disease is associated with a disorder of insulin- or contraction-induced glucose metabolism in a skeletal muscle cell *in vivo*.[3,4] Such a bioassay system could be also useful for screening candidate drugs against type 2 diabetes.

Bioassay systems fabricated by combining microelectric devices with cell-micropatterning techniques have enabled localized electrical regulation and long-term monitoring of electrophysiological responses from cells such as neural, cardiac, and skeletal muscle cells cultured on the device.[5–12] However, it is difficult to culture fully differentiated cells and to maintain their physiological activity on the solid devices. Specifically, there are few reports on devices combined with electrically excitable contractile skeletal muscle cell culture because the cells readily detached from the substrate within a few days.[13] For a stable bioassay device, it is necessary to develop an on-device culture method of fully differentiated cells, while sustaining their activity for long periods.

Recently, to overcome the difficulties associated with on-device cultivation, a manipulatable cell sheet which is composed of confluent cell monolayers and a flexible polymer sheet has been developed.[14–17] The cell sheet can be handled while sustaining the cellular structure and activity and it can be combined with the devices on demand. We have developed gel sheet-supported contractile C_2C_{12} myotube micropatterns by means of the cell transfer technique (Fig. 1(A)).[17] Micropatterned myotubes/gel sheet was prepared by transferring the myotube line patterns cultured on a glass substrate onto the surface of fibrin gel sheet with 100% efficiency. Myotubes on the gel sheet exhibited longer-term contractile activity without detachment from the gel than the cells on a conventional solid culture dish.

In the present study, we patched the myotube/fibrin gel sheet onto a microelectrode array chip to construct a skeletal muscle cell-based bioassay device (Fig. 1(B)). The Pt microelectrode arrays were previously coated with a conducting polymer, poly(3,4-ethylenedioxythiophene) (PEDOT), that has a large electroactive surface area due to its fibrous structure. This modification increases the interfacial electrical capacity of the electrodes and ensures a less invasive electrical stimulation of the cells without causing faradaic reactions and gas evolution.[18]

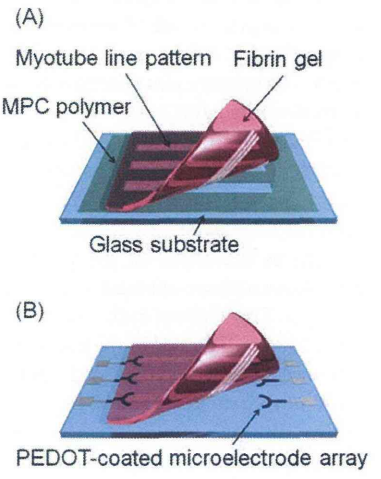

Fig. 1 Overview of the myotube/fibrin gel sheet combined with the PEDOT microelectrode array chip. (A) Cell transfer from a glass substrate to a fibrin gel. (B) Attachment of the myotube/fibrin gel onto the microelectrode arrays.

[a]*Department of Bioengineering and Robotics, Graduate School of Engineering, Tohoku University, 6-6-01 Aramaki, Aoba-ku, Sendai, 980-8579, Japan. E-mail: nishizawa@biomems.mech.tohoku.ac.jp; Fax: +81 22 795 7003; Tel: +81 22 795 7003*
[b]*JST-CREST, Sanbancho, Chiyoda-ku, Tokyo, 102-0075, Japan*
[c]*Department of Biomedical Engineering, Graduate School of Biomedical Engineering, Tohoku University, Biomedical BLD, 2-1 Seiryo-machi, Aoba-ku, Sendai, 980-8575, Japan*

† Electronic supplementary information (ESI) available: Movie 1 and 2. See DOI: 10.1039/c0lc00364f

The usefulness of this device for type 2 diabetes researches was demonstrated by fluorescent imaging of the contraction-induced translocation of the glucose transporter, GLUT4, from intracellular vesicles to the plasma membrane of the myotubes. GLUT4 is a principal mediator of glucose uptake in the skeletal muscle cell in response to insulin and contraction. GLUT4 distributes in the intracellular region under unstimulated state, and is transported to the plasma membrane in response to these stimuli to accelerate glucose uptake in the cells. Defection in stimuli-responsive GLUT4 translocation is closely associated with the development of type 2 diabetes, which is supported by the whole animal experiments.[3,4]

Experimental

Contractile C_2C_{12} myotube micropatterns on a fibrin gel

Wild type (WT)-C_2C_{12} myoblasts (less than six passages in age; American Type Culture Collection, Manassas, VA, USA) were cultured on a glass substrate with a line-patterned cell-resistant polymer, 2-methacryloyloxyethyl phosphorylcholine (MPC, Lipidure-CM5206E, NOF Corp., Tokyo, Japan) at 37 °C, under a 5% CO_2 atmosphere in a growth medium composed of Dulbecco's modified Eagle's medium (DMEM, Wako Pure Chemicals Industries, Ltd, Osaka, Japan) containing 10% fetal bovine serum (BioWest, Nuaille, France), 100 units mL^{-1} penicillin, and 100 μg mL^{-1} streptomycin (Invitrogen Corp., Carlsbad, CA, USA) until fully confluent. Myoblasts were induced to differentiate into myotubes by replacing the growth medium with a differentiation medium composed of DMEM containing 2% calf serum (Thermo Electron Corporation, Melbourne, Australia), 1 nM insulin (Sigma-Aldrich, St Louis, MO, USA), 100 units mL^{-1} penicillin, and 100 μg mL^{-1} streptomycin.

Then, the myotubes were transferred onto a fibrin gel. The fibrinogen mixture solution was prepared by dissolving 15 mg mL^{-1} fibrinogen (Sigma-Aldrich), 0.5 mg mL^{-1} aprotinin (Sigma-Aldrich), and 10 U mL^{-1} thrombin (Ito Life Science, Inc., Ibaraki, Japan) in an electrical pulse stimulation (EPS) medium composed of DMEM containing 2% calf serum, 2% MEM amino acids solution (Invitrogen Corp.), 1% MEM non-essential amino acids solution (Invitrogen Corp.), 100 units mL^{-1} penicillin, and 100 μg mL^{-1} streptomycin. The mixture was poured over the cells, and the culture was left undisturbed for 2 h at 37 °C under a 5% CO_2 atmosphere to facilitate fibrin gelation and to allow the cells to adhere on the surface of the gel. Fig. 2(A) shows a photograph of the fibrin gel sheet (size, 1 cm × 1 cm; thickness, 2 mm) with myotube line patterns after detaching the gel from the substrate. The white lines seen at the center of the gel are myotube line patterns. Fig. 2(B) shows a phase-contrast micrograph of myotube line patterns on the gel. The width of each line and the gap between the lines were set at 250 μm. The side of the fibrin gel sheet with the attached myotubes was covered with an additional thin fibrin gel layer (less than 100 μm) because we found that the additional gel layer was effective for maintaining the structure of cellular micropatterns for a long term. The myotube/fibrin gel was finally placed in a carbon electrode chamber (C-Pace 100, IonOptix, Milton, MA, USA) and periodic electrical pulses (amplitude, 0.7 V mm^{-1}; frequency, 1 Hz; duration, 2 ms) were applied for 4 days in the EPS medium to endow the cells with contractile activity.[17]

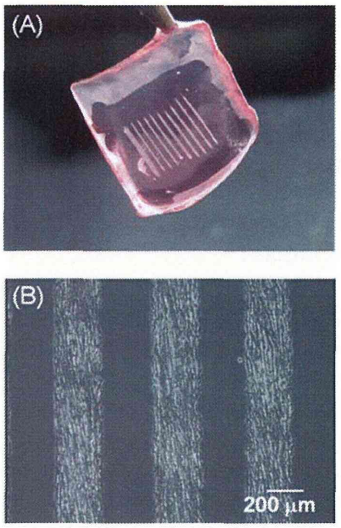

Fig. 2 (A) Photograph of a fibrin gel with myotube line patterns. (B) Phase-contrast micrograph of myotube line patterns on the gel.

Conducting polymer-coated Pt microelectrode arrays

Pt microelectrode arrays were fabricated on a glass substrate using conventional photolithography and lift-off techniques. Electropolymerization of poly(3,4-ethylenedioxythiophene) (PEDOT) on the microelectrode surfaces was carried out for 1 min in an aqueous solution containing 50 mM 3,4-ethylenedioxythiophene (Sigma-Aldrich) as a monomer and 100 mM KNO_3 as a dopant under potentiostatic conditions at +1.0 V *vs.* Ag/AgCl. Thickness of the PEDOT layer on the electrode was 467 ± 22 nm (n = 5) measured using a surface profiler (P-10, KLA-Tencor, CA, USA).

The contractile myotube/fibrin gel sheet was placed on the PEDOT microelectrode arrays so that the side of the gel sheet with the attached myotubes was in contact with the electrode surface. The myotube line patterns were carefully aligned with the microelectrode patterns using tweezers under microscopic observation. Periodic electrical pulses were applied between the desired microelectrode pairs to induce myotube contraction in the EPS medium.

GLUT4 translocation assay by immunostaining

Transfected C_2C_{12} myotube stably expressing rat GLUT4, with a c-myc epitope tag in the first extracellular loop and an enhanced cyan fluorescent protein (ECFP) at the carboxyl terminus, was used to detect membrane-bound GLUT4 using an anti-c-myc antibody.[19,20] WT- and transfected myoblasts mixed at a 1 : 1 ratio were grown and differentiated on a MPC polymer patterned substrate[19,20] and transferred onto a fibrin gel as described above. The myotubes were electrically stimulated using the carbon electrode chamber for 4 days to endow the cells with contractile activity. Then, the gel sheet was placed on the PEDOT microelectrode arrays for localized electrical stimulation of arbitral myotube line pattern for 3.5 h (amplitude, 2 V; duration, 3 ms; frequency, 10 Hz; train, 1 s; interval, 10 s) in the EPS medium. After that, the cells were fixed with 1% *p*-formaldehyde (Electron Microscopy Sciences, Fort Washington, PA,